

# Collective evolution of a parton in the vacuum: the ultimate partonic “droplet”, non-perturbative QCD and quantum entanglement

Austin Baty,<sup>1</sup> Parker Gardner,<sup>1</sup> and Wei Li<sup>1</sup>

<sup>1</sup>*Physics and Astronomy Department, Rice University, Houston, Texas 77005, USA*

We postulate that non-perturbative QCD evolution of a single parton in the vacuum will develop the long-range collective effects of a multi-parton system, reminiscent of those observed in high-energy hadronic or nuclear interactions with large final-state particle multiplicity final-state particles. Proton-Proton collisions at the Large Hadron Collider showed surprising signatures of a strongly interacting, thermalized quark-gluon plasma, which was thought only to form in collisions of large nuclear systems. Another puzzle observed earlier in  $e^+e^-$  collisions is that production yields of various hadron species appear to follow a thermal-like distribution with a common temperature. We propose searches for thermal and collective properties of a single parton propagating in the vacuum using high multiplicity jets in high-energy elementary collisions. Several observables are studied using the PYTHIA 8 Monte Carlo event generator. Experimental observation of such long-range collectivity will offer a new view of non-perturbative QCD dynamics of multi-parton systems at the smallest scales. Absence of any collective effect may offer new insights into the role of quantum entanglement in the observed thermal behavior of particle production in high energy collisions.

## I. INTRODUCTION

Quantum Chromodynamics (QCD) is the fundamental theory that describes properties of quarks and gluons (known as partons) and the interactions among them. Being an  $SU(3)$  non-abelian gauge theory, QCD has the peculiar feature that partons interact strongly at long distances, but become almost free when close to each other (“asymptotic freedom”) [1–3]. As a consequence, no free partons are ever found in the vacuum. Instead, partons are always confined inside hadrons. Attempts to knock a parton out of a hadron and into the vacuum (e.g., via a hard scattering in high-energy proton collisions) lead to the emission of collimated sprays of hadrons (or “jets”) that result from fragmentation and hadronization of the scattered parton. During this process, the parton acquires “mass” or “virtuality” via interactions with the vacuum. Detailed dynamics of the parton fragmentation and hadronization process are not yet fully understood and cannot be evaluated from first-principles because of QCD’s non-perturbative nature. Phenomenological models such as the Lund string [4] and cluster models [5] have been implemented to facilitate the interpretation of experimental data. In recent years, applications of perturbative QCD have been successful in the study of jet substructures, where non-perturbative components (i.e., soft particles) of the jet are largely trimmed away [6]. Fundamental understandings of *color confinement* and the *dynamics of hadronization* are two key outstanding issues in QCD and strong interactions.

Experiments studying high-energy heavy nucleus collisions have been carried out to overcome the QCD confinement and create (possibly thermalized) matter with quark-gluon degrees of freedom over an extended space-time dimension. Lattice QCD theory predicts that a crossover transition to a new phase of partonic matter, known as the *quark-gluon plasma* (QGP), occurs at a temperature of about 157 MeV near zero baryon chem-

ical potential [7–9]. In a high-energy nucleus-nucleus ( $AA$ ) collision (e.g., Au or Pb ion), the large volume and density of initial partons can lead to many rescatterings, which may rapidly drive the system toward a thermalized QGP state. Over the past decades, experiments at CERN’s Super Proton Synchrotron (SPS) [10], BNL’s Relativistic Heavy Ion Collider (RHIC) [11–14], and CERN’s Large Hadron Collider (LHC) [15] have provided compelling evidence for the formation of hot and dense QGP matter. Striking long-range collective phenomena have been observed and extensively studied using the azimuthal correlations of particles emitted over a wide pseudorapidity range (also known as the “Ridge”) at RHIC [16–19] and the LHC [20–24]. These observations indicate that QGP matter is strongly coupled and exhibits the hydrodynamic behavior of a nearly perfect liquid [25–29].

It was thought that elementary collision systems such as  $e^+e^-$ , proton-proton etc. were too small and dilute for any secondary partonic rescattering to occur and drive the system toward equilibrium. For this reason, collective flow behavior from a QGP medium was not expected in these systems. Surprisingly, since the start of the LHC, similar long-range collective azimuthal correlations have been discovered in proton-proton (pp) collisions with large final-state particle multiplicity [30–34], which raised the question of whether a tiny QGP droplet with a significantly smaller size is created [35]. Subsequently, such collective phenomena have been observed in additional small systems, such as proton-nucleus ( $pA$ ) [36–45] and lighter nucleus-nucleus systems [45–48] at RHIC and the LHC. While it is widely accepted that strong final-state partonic rescatterings do play a prominent role in the observed collectivity of small, high-multiplicity systems, questions remain whether the rescatterings are strong enough to drive the system close to equilibrium or a domain where hydrodynamics is applicable. Meanwhile, alternative scenarios based on gluon saturation in the initial state may also contribute, especially at lower par-

ticle multiplicities (see reviews and latest developments in Refs. [49–51]).

It is evident that collective effects of strongly correlated partonic systems are not only limited to those created in large  $AA$  collisions. Therefore, a series of compelling questions arise: *From how small of a system can partonic collectivity emerge and under what conditions? Is partonic collectivity at such small scales unexpected or a natural consequence of QCD in its non-perturbative regime? Can hydrodynamics be an effective tool in describing non-perturbative QCD dynamics of many-body partonic systems (e.g., fragmentation in the vacuum)?*

In fact, it has been pointed out long ago that total production yields of various hadron species in elementary  $e^+e^-$  collisions can be well described by a thermal statistical model [52–54], similar to that in large  $AA$  collisions from a nearly thermalized QGP medium [55]. The origin of this thermal-like phenomenon in  $e^+e^-$  has not been understood, as it was inconceivable that strong final-state partonic rescatterings occur there. Searches for long-range ridge correlations in  $e^+e^-$  [56] or  $e^-p$  collisions [57] have also yielded null results so far, although the event multiplicity reached is rather limited (up to  $\sim 30$  charged particles). There are conjectures that thermal-like hadron production is the QCD counterpart of Hawking-Unruh radiation [54, 58, 59].

In recent years, quantum entanglement effects were proposed to give an intriguing alternative perspective of multi-particle production in high-energy collisions. [60–64]. The apparent thermalization of final-state hadrons in  $e^+e^-$  may be related to dynamics of an expanding quantum string stretched between the quark–antiquark pair and its subsequent quenching [61]. No secondary partonic scatterings are involved in this explanation. In these models entanglement entropy is calculated with an effective thermal temperature and can be related to the temperature extracted by fitting identified hadron multiplicities to thermal statistical models.

Motivated by earlier experimental and theoretical work, our purpose in this paper is to discuss the possibility of understanding the fundamental questions and puzzles outlined above from a different view. *In particular, we postulate that a strongly-interacting, QGP-like state<sup>1</sup> can indeed be formed by a system as small as a single quark or gluon as it propagates through the QCD vacuum.* As a natural consequence of the intrinsic strong QCD coupling strength, the strong color fields of the primordial parton in the vacuum can excite a large number of secondary partons. These partons subsequently interact and develop collective expansion which is transverse to the original parton’s direction of motion and extends over a finite space-time volume. We lay out the proposal to examine a series of key signatures (e.g., long-range

azimuthal correlations) of such single-parton, QGP-like states using energetic jets copiously produced in  $pp$  collisions at the present CERN-LHC, and also at potential future colliders of  $pp$ ,  $e^-p$  and  $e^+e^-$ . Similar studies are also applicable in nuclear collisions to explore the “expansion” of a parton in a colored medium formed there, instead of vacuum. Observation of QGP-like signatures for a single parton will provide new insights to the “thermal” behavior seen from  $e^+e^-$  to  $AA$  collisions, and offer a unified view of non-perturbative many-body QCD processes (e.g., hydrodynamics models). Conversely, absence of those collective signatures may highlight the role of quantum entanglement effects in parton fragmentation and hadronization.

The paper is organized in the following way: Section II outlines the underlying idea of the possible formation of “QGP” in a parton propagating in the vacuum. Section III discusses specific key signatures and how to search for them experimentally using Monte Carlo (MC) generators for demonstration. Section IV is devoted to more physics discussions and extension of proposed studies to other future directions. The paper ends with a summary in Section V.

## II. SINGLE-PARTON “QGP” IN THE VACUUM

In the QCD vacuum state, the chiral symmetry is spontaneously broken because of the strong coupling nature at low energies. The QCD vacuum is not empty but filled with non-vanishing condensates of quark-antiquark pairs ( $\langle\bar{q}_L q_R\rangle + \langle\bar{q}_R q_L\rangle$ ) and gluons ( $\langle G_{\mu\nu} G^{\mu\nu}\rangle$ ), or chiral condensates. Consider an extreme (although unrealistic) situation, where a single parton is placed at rest in the vacuum, as illustrated in Fig. 1 (top). The potential energy of associated color fields is infinite. Consequently, more quarks and gluons will be immediately excited out of the surrounding condensate sea. A local, dense partonic system is then formed and may develop strong rescatterings and exhibit collective expansions until the energy density drops and partons are grouped into hadrons. Such a process is essentially reminiscent of the evolution of a QGP liquid created in a nuclear collision.

Clearly, the kind of initial conditions depicted in Fig. 1 (top) are not possible to set up experimentally. Now we consider more realistic scenarios, where a parton (or partons) is knocked out of a proton into the vacuum in hard scattering processes of  $pp$  collisions. This scenario is equivalent to the case of a stationary parton in the vacuum if it is Lorentz-boosted to a fast-moving frame, as illustrated in Fig. 1 (lower). In this case, the struck parton carrying strong color fields will be “colliding” into the vacuum chiral condensates along its passage and locally excite multiple partons, which undergo strong rescatterings and develop QGP-like collective expansion in the transverse plane to the moving-parton direction. The process will last until the primordial parton loses all its energy. Experimentally, such a parton will end

<sup>1</sup> “QGP-like” refers to the state where qualitative signatures of partonic collectivity are present but the system does not necessarily reach the hydrodynamic limit.

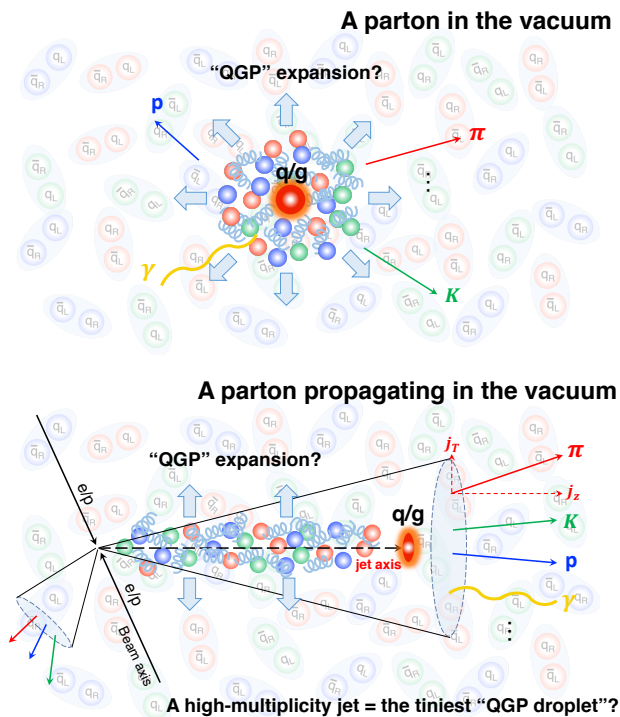


FIG. 1. Cartoons of a single parton evolving at rest in the vacuum (left) and fast-moving through the vacuum (right).

up being observed as a “jet”, a spray of hadrons, and it gains a “mass” via interactions with the vacuum. High-multiplicity jets would correspond to the fluctuation of a parton interacting with a large number of vacuum condensates, and acquiring large “mass” or “virtuality”. The process of parton fragmentation into hadrons has been studied extensively in collider experiments. Because of its nonperturbative nature, parton fragmentation cannot be rigorously calculated in QCD. Phenomenological models such as the Lund string model [4] are often employed albeit with limited success (i.e., many tuning parameters). Studies of jet substructures in recent years [6] have offered great insights into our understanding of the parton fragmentation process. However, lots of techniques developed based on perturbative QCD tend to trim away soft-radiated particles where intriguing collective QCD phenomena may occur. Our goal in this paper is to focus on studying soft particle production with respect to the jet axis, and particularly searching for thermalization and collective expansion effects (such as radial and elliptic flow as will be discussed in detail later). These effects are particularly likely to develop in high-multiplicity jets, where the primordial parton presumably undergoes many rescatterings.

The analysis strategy discussed in this paper is universally applicable to any high-energy collision system including  $pp$ ,  $e^+e^-$  and  $e^-p$ , where energetic jets (often dijets) are copiously produced. High transverse momentum (relative to the beam axis) jets are first reconstructed in

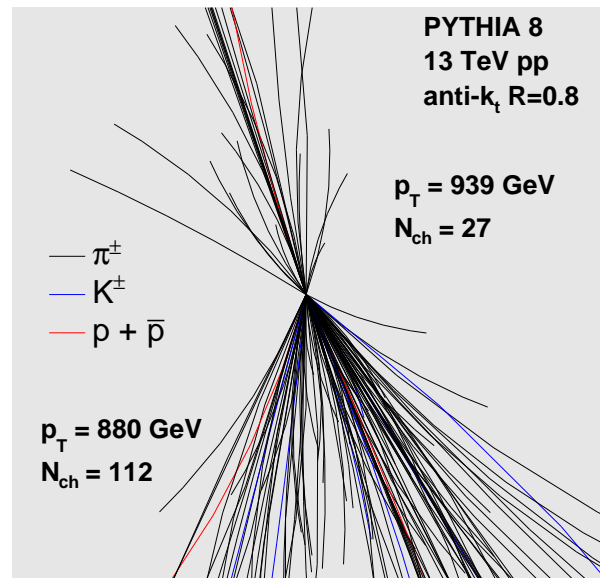


FIG. 2. A simulated event display for a PYTHIA 8 dijet event in the transverse plane with a weak axial magnetic field. One of the two jets has a high multiplicity of charged particles ( $N_{\text{ch}}^j$ ), found by the anti- $k_t$  algorithm with a cone size of  $R=0.8$ . Other particles not assigned to the two main jets by the jet finding algorithm (e.g., from the underlying event) are not shown.

an event using a particular algorithm (e.g., anti- $k_t$  [65]) with a choice of jet cone size. For an individual jet we define a new coordinate frame such that the  $z$ -axis is aligned with the direction of jet momentum, named the *jet frame*, as illustrated in Fig. 1. Momentum vectors of all particles found within the jet cone are then re-defined in this new frame,  $\vec{p}^* = (j_T, \eta^*, \phi^*)$ . Here,  $j_T$  is the particle transverse momentum with respect to the jet axis. By selecting very high  $p_T$  jets, effects of particles from the underlying event that coincidentally fall inside the jet cone can be significantly suppressed. We then propose to study a wide range of key QGP signatures, observed in  $AA$  collisions, for particles produced inside high- $p_T$  jets under this new frame as a function of charged multiplicity inside the jet cone, denoted as  $N_{\text{ch}}^j$ . In the following Section III, we present results on a number of observables studied using the PYTHIA 8 Monte Carlo (MC) event generator [66]. As no effects of rescatterings among produced parton showers or strings are expected for the parton fragmentation process in PYTHIA 8 (or any other MC event generator presently on the market), our MC studies provide a baseline for demonstrating the ideas of how to search for key signatures with experimental observables.

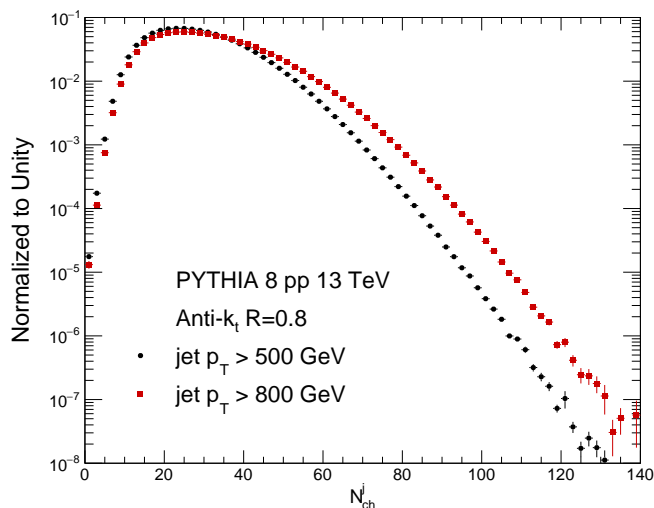


FIG. 3. Charged multiplicity distributions of jets with  $p_T > 500$  GeV and  $800$  GeV, respectively. Jets are found by the anti- $k_t$  algorithm with a cone size of  $R=0.8$ .

### III. SEARCH FOR SIGNATURES OF SINGLE-PARTON “QGP” DROPLET

We first investigate some basic properties of particles produced within a jet in the new frame. As an illustration of the type of events that are being selected in this analysis, a sample PYTHIA 8 dijet event of  $pp$  collisions at  $\sqrt{s} = 13$  TeV is shown in Fig. 2, in the transverse plane of the lab frame. The display perspective is along a weak axial magnetic field, which causes the charged particles to bend in arcs. The two jets are produced and reconstructed with the anti- $k_t$  [65] algorithm of cone size  $R=0.8$ , each having  $p_T$  of roughly  $900$  GeV. The first jet has a fairly average multiplicity of  $27$ , while the second jet has over 4 times as many charged particles, and would be classified as ‘high multiplicity’. Different colors of particle trajectories indicate different particle species, such as pions, kaons and protons. Jets reconstructed with smaller cone sizes (e.g.,  $R=0.4$ ) are also investigated and show qualitatively similar properties of observables studied in this paper so we focus on presenting results only for jet cone size of  $0.8$ . The PYTHIA sample used in this study corresponds to an integrated luminosity of approximately  $50 \text{ fb}^{-1}$  and is filtered to select events having a minimum invariant transverse momentum ( $\bar{p}_T$ ) of  $470$  GeV.

Figure 3 shows multiplicity distributions of charged particles within an AK8 (anti- $k_t$  reconstruction of cone size  $R=0.8$ ) jet of  $p_T > 500$  GeV and  $p_T > 800$  GeV in PYTHIA 8. The most likely values of charged particle multiplicity are around  $25$  for both jet  $p_T$  selections, but the distribution for higher- $p_T$  jets has a slightly longer tail at higher multiplicities, reaching up to  $140$  charged particles. This can be understood as the higher jet momentum causes more produced particles to fall within the jet cone because of the larger Lorentz boost asso-

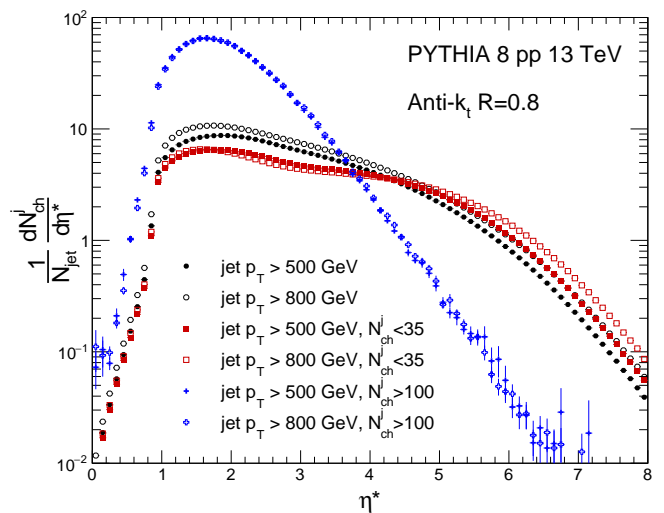


FIG. 4. The pseudorapidity ( $\eta^*$ ) distributions of charged particle densities in the single jet frame for low ( $N_{\text{ch}}^j < 35$ )- and high ( $N_{\text{ch}}^j > 100$ )-multiplicity jets with  $p_T > 500$  GeV and  $800$  GeV, respectively. Jets are found by the anti- $k_t$  algorithm with a cone size of  $R=0.8$ .

ciated with the increased parton momentum. However, the difference between the two selections for a given multiplicity probability is only around  $10$  charged particles at high multiplicities, indicating only a loose correlation between jet  $p_T$  and multiplicity, which is also observed in experimental data at sufficiently high jet  $p_T$  [67]. Given that high-multiplicity jets are rarely produced and that they are only loosely correlated with jet  $p_T$ , suggested by Fig. 3, standard  $p_T$ -based experimental online triggers are not optimal for studying these systems, and a dedicated trigger filtering on high multiplicities from a single jet will significantly enhance the potential of searching for new phenomena.

Distributions of charged particle densities in pseudorapidity of the jet frame,  $dN_{\text{ch}}/d\eta^*$ , within an AK8 jet are shown in Fig 4. In the jet coordinate system, low  $\eta^*$  corresponds to particles that are separated from the main jet axis by a large angle, while high  $\eta^*$  corresponds to particles more collimated with the jet direction. The closed points show distributions for jet  $p_T > 500$  GeV, while open points correspond to  $p_T > 800$  GeV. An inclusive multiplicity selection is shown in black, while low ( $N_{\text{ch}}^j < 35$ ) and high ( $N_{\text{ch}}^j > 100$ ) multiplicity selections are shown in red and blue, respectively.

The distribution tends to shift towards lower values of  $\eta^*$ , i.e. large emission angles for the high multiplicity selection, as compared to the inclusive and low multiplicity selections. This is consistent with higher-multiplicity jets being more likely to be initiated by a gluon scattering, where emitted particles are less collimated along the jet direction. All three selections have a very sharp rising trend around  $\eta^* = 0.86$  which is related to the angle the particle makes with respect to the jet axis being near the chosen cone size of  $0.8$ . For the high multiplicity se-

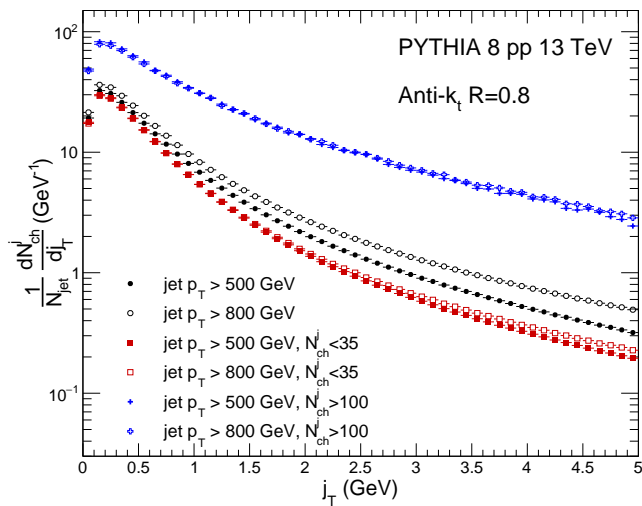


FIG. 5. The  $j_T$  distributions of charged particles in the single jet frame for low ( $N_{\text{ch}}^j < 35$ )- and high ( $N_{\text{ch}}^j > 100$ )-multiplicity jets with  $p_T > 500$  GeV and 800 GeV, respectively. Jets are found by the anti- $k_t$  algorithm with a cone size of  $R=0.8$ .

lection, the  $dN_{\text{ch}}/d\eta^*$  reaches values of nearly 70, which is comparable to the multiplicity regime where collective effects have been observed in high-multiplicity  $pp$  collisions [30–33]. Therefore, it is feasible to expect that similar multi-parton dynamics may be developed inside a jet of sufficiently high multiplicity. Unlike in  $pp$  and  $AA$  collisions where there is a wide plateau region in  $dN_{\text{ch}}/d\eta$  over a few units, the  $\eta^*$  distribution of a single jet is much narrower, especially at large multiplicities. Figure 5 shows  $j_T$  distributions of charged particle yields for two different jet  $p_T$  selections and multiplicity selections. All selections exhibit a sharp peak at low  $j_T$  values, but the tail of the low-multiplicity selection falls off slightly faster than the inclusive selection. This is consistent with particles in these jets being emitted as narrower angles relative to the jet axis on average, as was already observed in the  $dN_{\text{ch}}/d\eta^*$  distribution. The distributions for the high-multiplicity selection are remarkably similar for both jet  $p_T$  choices.

In the following subsections, we employ the PYTHIA 8 generator as a baseline to investigate a series of observables relevant to signatures of a QGP and explore potential discoveries in future experiments. The list of observables is not exhaustive but rather representative of several selected key signatures:

- Particle multiplicity and *strangeness enhancement* in a dense, thermal partonic medium;
- Long-range correlations and *anisotropy flow*;
- *Radial flow* boost to identified particle  $j_T$  spectra;
- *Quantum Interference* of identical particles;

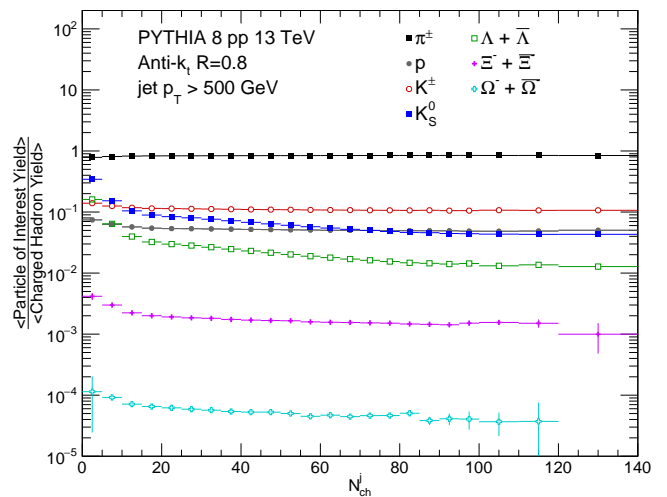


FIG. 6. Ratios of total yields of various hadrons to inclusive charged hadrons from AK8 jets for jet  $p_T > 500$  GeV, as a function of charged multiplicity in jet ( $N_{\text{ch}}^j$ ), in PYTHIA 8  $pp$  events at  $\sqrt{s} = 13$  TeV.

### A. Particle Multiplicity and Strangeness Enhancement

We propose to study the total multiplicity of each particle species and their relative ratios for particles produced from a single jet in a similar fashion to those in other collision systems. Statistical models can also be used to describe the particle multiplicity data in jets to search for evidence of thermal production from a single parton that may be related to the quantum entanglement effect or a strongly interacting medium. In the analysis presented here, we specifically focus on the aspect of strange hadron multiplicities and explore possible strangeness enhancement phenomena as a function of the charged multiplicity in jets, using the PYTHIA 8 model.

The enhancement of strange hadron production (relative to non-strange hadrons) in  $AA$  collisions has been considered as strong evidence for the existence of a high-gluon density QGP medium, where the gluon splitting channel dominates the strangeness production [68]. In recent years, it has also been observed that in small  $pp$  and  $pA$  systems, strange hadron yields relative to pions smoothly increase as higher multiplicity events are selected [69] toward multiplicity values in  $AA$  collisions. The PYTHIA 8 model is unable to reproduce the observed strangeness enhancement in  $pp$  collisions.

We propose to explore similar strangeness enhancement phenomena in high  $p_T$  jets, as a function of jet multiplicity. Using PYTHIA 8 as a reference, Fig. 6 shows the ratio of various light and strange hadron yields in a high- $p_T$  ( $> 500$  GeV) AK8 jet to those of charged pions, as a function of the charged multiplicity of a jet ( $N_{\text{ch}}^j$ ). As expected, no strangeness enhancement is observed in PYTHIA 8. The ratios of protons to pions is nearly constant as a function of  $N_{\text{ch}}^j$ . For strange hadrons

such as kaons,  $\Lambda$ ,  $\Xi^-$ , and  $\Omega^-$ , a slight downward trend is observed for  $N_{\text{ch}}^j$  values less than 20, but the ratio is nearly independent of multiplicity above this threshold. Observation of an increasing strange particle-to-pion yield ratio experimentally in high-multiplicity jets would be a compelling indication of additional physics not captured by the canonical fragmentation and/or hadronization model via string breaking, but possibly involving dynamics of dense gluon interactions such as those in high-multiplicity  $pp$ ,  $pA$  and  $AA$  collisions.

## B. Long-Range Correlations and Anisotropy Flow

Long-range collective phenomena over a wide pseudorapidity range have been observed in azimuthal correlations of particles from a variety of collision systems and experiments. In particular, the persistence of these collective phenomena in increasingly small systems has lead to debates about the origin of such behavior and the development of new experiments to push the limits of hydrodynamic validity and explore possible effects of quantum entanglement.

We briefly describe the analytical steps of two-particle angular correlation analyses in the jet frame and discuss key features of the result. The procedure is similar to that employed in Ref. [36], except that the momentum vector of all particles are re-defined in the jet frame. The 2-D angular correlation function is calculated as follows:

$$\frac{1}{N_{\text{ch}}^{\text{trg}}} \frac{d^2 N^{\text{pair}}}{d\Delta\eta^* d\Delta\phi^*} = B(0,0) \frac{S(\Delta\eta^*, \Delta\phi^*)}{B(\Delta\eta^*, \Delta\phi^*)}. \quad (1)$$

where  $\Delta\eta^*$  and  $\Delta\phi^*$  are relative pseudorapidity and azimuthal angle in the jet frame, for a pair of trigger and associate particles. The trigger and associate particles can be selected from the same or different  $j_{\text{T}}$  ranges. For analyses presented below, trigger and associate particles are chosen from the same  $j_{\text{T}}$  range for simplicity. The correlation functions are typically measured in different  $j_{\text{T}}$  and multiplicity ranges.

The  $S(\Delta\eta^*, \Delta\phi^*)$  and  $B(\Delta\eta^*, \Delta\phi^*)$  represent the signal and background distributions, respectively:

$$S(\Delta\eta^*, \Delta\phi^*) = \frac{1}{N_{\text{ch}}^{\text{trg}}} \frac{d^2 N^{\text{sig}}}{d\Delta\eta^* d\Delta\phi^*}, \quad (2)$$

and

$$B(\Delta\eta^*, \Delta\phi^*) = \frac{1}{N_{\text{ch}}^{\text{trg}}} \frac{d^2 N^{\text{bkg}}}{d\Delta\eta^* d\Delta\phi^*}. \quad (3)$$

The signal distribution is calculated with pairs taken from each jet ( $N^{\text{sig}}$ ) and then averaged over all jets, weighted by the jet multiplicity. The background distribution serves as a reference and a correction to the pair acceptance due to limited  $\eta^*$  range. To construct the background distribution, we first derive the 2-D

single-particle  $\eta^*$ - $\phi^*$  distribution for daughters of all jets. Pseudo-particles are then randomly drawn from the  $\eta^*$ - $\phi^*$  distribution. These pseudo-particles are built from values accumulated over multiple distinct jets in multiple distinct events. In this way, no correlations should exist in the background distribution and all features are detector-related. A large number of pseudo-particles  $n_{\text{pseudo}}$  are created such that  $N_{\text{bkg}} = n_{\text{pseudo}}(n_{\text{pseudo}} - 1)/2 \approx 10 \times N_{\text{sig}}$ , where  $N_{\text{sig}}$  is the total number of entries in the complete signal distribution for the class. The  $B(0,0)/B(\Delta\eta^*, \Delta\phi^*)$  term is the appropriate bin-by-bin correction to the signal distribution.

Figure 7 shows the 2-D two-particle angular correlation function for low- and high-multiplicity jets and particles with  $0.3 < j_{\text{T}} < 3$  GeV in PYTHIA 8  $pp$  collisions at 13 TeV. The central peak at  $(\Delta\eta^*, \Delta\phi^*) = (0,0)$  is the result of short-range correlations from local parton shower and hadronization. The far-side ridge at  $\Delta\eta^* \approx \pi$  is mostly related back-to-back particle production by conservation of momentum. These prominent features have been found in lab-frame analyses for both experimental data and MC simulations. Moreover, another feature commonly observed in  $AA$  collisions is the near-side enhancement at  $\Delta\phi^* \approx 0$  over long-range in  $\Delta\eta^*$ , commonly known as the near-side ‘‘ridge’’. The persistence of this ridge to very small systems, such as  $pp$  and  $pA$  collisions, naturally motivates a proposal to continue searching for these effects in even smaller systems, like a single jet. As expected, there is no indication of a near-side ridge for both low- and high-multiplicity jets in PYTHIA 8. This is also consistent with  $e^+e^-$  [56] and  $e^-p$  collisions [57] at relatively low final-state multiplicity.

The resulting 2-D distribution can be further understood by decomposition into a 1-D Fourier series of projections along the  $\Delta\phi^*$  axis:

$$\frac{1}{N_{\text{ch}}^j} \frac{dN^{\text{pair}}}{d\Delta\phi^*} \propto 1 + 2 \sum_{n=1}^{\infty} V_{n\Delta}(j_{\text{T}}^{\text{A}}, j_{\text{T}}^{\text{B}}) \cos(n\Delta\phi^*), \quad (4)$$

where  $j_{\text{T}}^{\text{A}}$  and  $j_{\text{T}}^{\text{B}}$  represent the  $j_{\text{T}}$  of trigger and associate particles, respectively. By taking 1-D  $\Delta\phi^*$  projections over  $\Delta\eta^* > 2$ , we exclude the short-range correlations and focus on understanding structure with large pseudorapidity separations. The strength of the Fourier components in such decomposition can give indications of the type of flow and its relative significance in various systems. The second Fourier component is typically associated with the strength of elliptical flow while the third is associated with the triangular flow.

In Fig. 8, 1-D  $\Delta\phi^*$  correlation functions for  $|\Delta\eta^*| > 2$  are shown for  $20 \leq N_{\text{ch}}^j \leq 30$  and  $N_{\text{ch}}^j \geq 70$ , respectively, for particles with  $0.3 < j_{\text{T}} < 3$  GeV from AK8 jets in PYTHIA 8  $pp$  collisions at 13 TeV. For both multiplicity classes, strong away-side correlations are observed, consistent with dominant contributions of momentum conservation. The near-side at  $\Delta\phi^* \sim 0$  shows a minimum, although there seems to be an indication of a slight enhancement for  $N_{\text{ch}}^j \geq 70$ . That enhancement is not significant

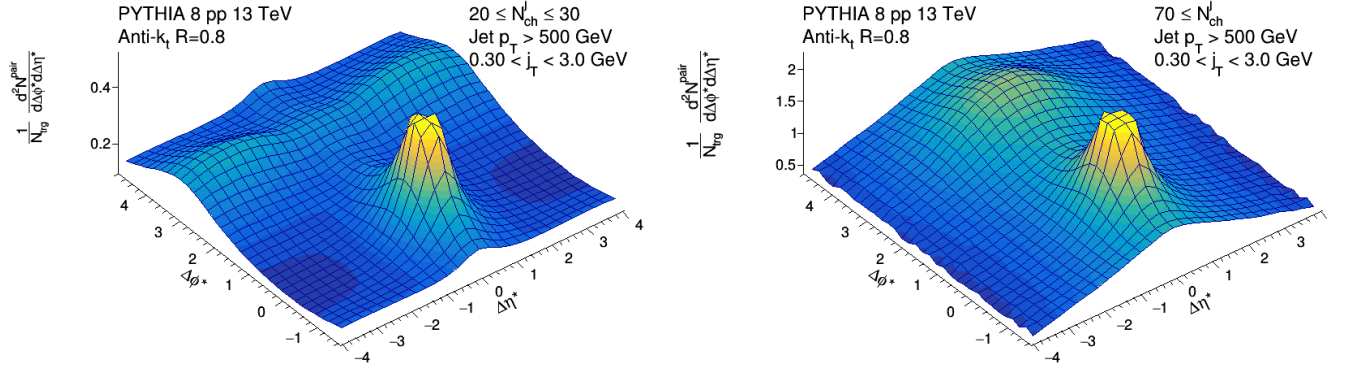


FIG. 7. The 2-D two-particle angular correlation functions for particle  $0.3 < j_T < 3$  GeV in low ( $20 \leq N_{\text{ch}}^j \leq 30$ , left) and high ( $N_{\text{ch}}^j \geq 70$ , right) in-jet charged multiplicity classes, for AK8 jets with jet  $p_T > 500$  GeV in PYTHIA 8  $pp$  events at  $\sqrt{s} = 13$  TeV.

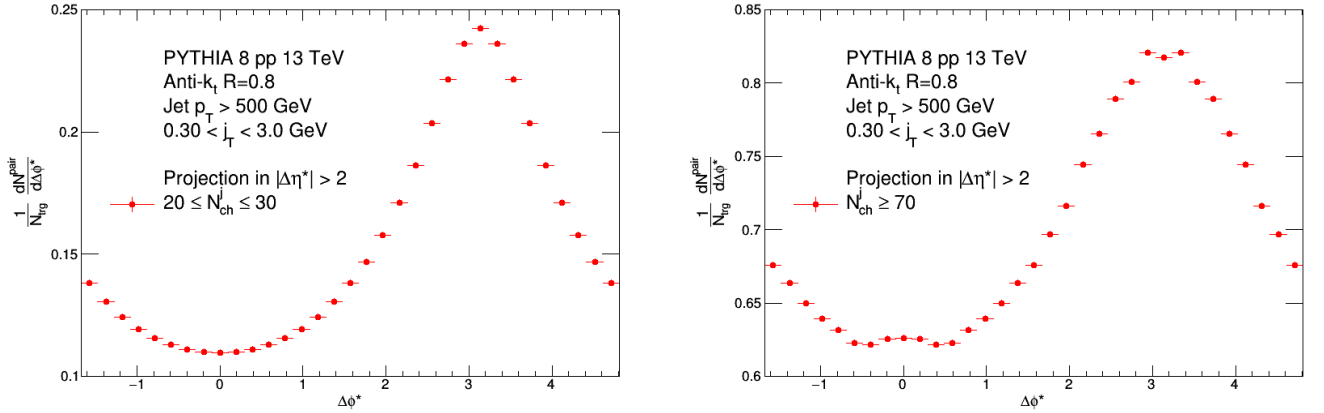


FIG. 8. The 1-D  $\Delta\phi^*$  two-particle angular correlation functions for particle  $0.3 < j_T < 3$  GeV and  $|\Delta\eta^*| > 2$ , in low ( $20 \leq N_{\text{ch}}^j \leq 30$ , left) and high ( $N_{\text{ch}}^j \geq 70$ , right) in-jet charged multiplicity classes, for anti- $k_t$   $R=0.8$  jets with jet  $p_T > 500$  GeV in PYTHIA 8  $pp$  events at  $\sqrt{s} = 13$  TeV.

and may also be related to the tail of short-range correlations at very large  $\Delta\eta^*$ .

Figure 9 shows the extracted two-particle Fourier coefficients,  $V_{n\Delta}$ , as a function of the charged multiplicity in jet ( $N_{\text{ch}}^j$ ), for the first three harmonic components, from AK8 jets in PYTHIA 8  $pp$  collisions at 13 TeV. Over the full  $N_{\text{ch}}^j$  range, the odd-order harmonics,  $V_{1\Delta}$  and  $V_{3\Delta}$ , are negative, while the even-order harmonics,  $V_{2\Delta}$  are positive. Magnitudes of all harmonics decrease as  $N_{\text{ch}}^j$  increases. All these features are consistent with expectation of short-range back-to-back correlations that are not related to collective effects. The contribution of short-range few-body correlation to the global azimuthal anisotropy of the event generally diminishes as  $1/N_{\text{ch}}^j$  in the two-particle Fourier coefficients. An increase of  $V_{2\Delta}$  or a significant positive  $V_{3\Delta}$  signal at very high multiplicity could be an indication of the onset of collective flow effects in the expansion of the parton jet. Note that the single-particle azimuthal anisotropy Fourier coefficient,  $v_n$ , is related to the two-particle Fourier coefficient as

$V_{n\Delta}(j_T^A, j_T^B) = v_n(j_T^A)v_n(j_T^B)$ . Dashed lines in Fig. 9 indicate values of  $V_{2\Delta}$  equivalent to 5%, 10% and 15% in single particle  $v_2$ . Therefore, if PYTHIA 8 properly models short-range correlations in the parton fragmentation process, a 15%  $v_2$  signal should be clearly identifiable with jets of  $N_{\text{ch}}^j > 70$ , while a much smaller  $v_2$  signal of about 5% would require pushing to much higher multiplicity jets, such as  $N_{\text{ch}}^j > 90-100$ .

### C. Identified Particle $j_T$ Spectra and Radial Flow

The hydrodynamic expansion of the QGP will generate a common velocity field that collectively boosts all produced particles along the radial expansion direction. This phenomena is known as the “radial flow” (see a review in Ref. [28]). As a consequence, final-state particles receive a push to higher average transverse momentum, with heavier particles gaining more momentum, proportional to the mass. This effect can be observed and quantified

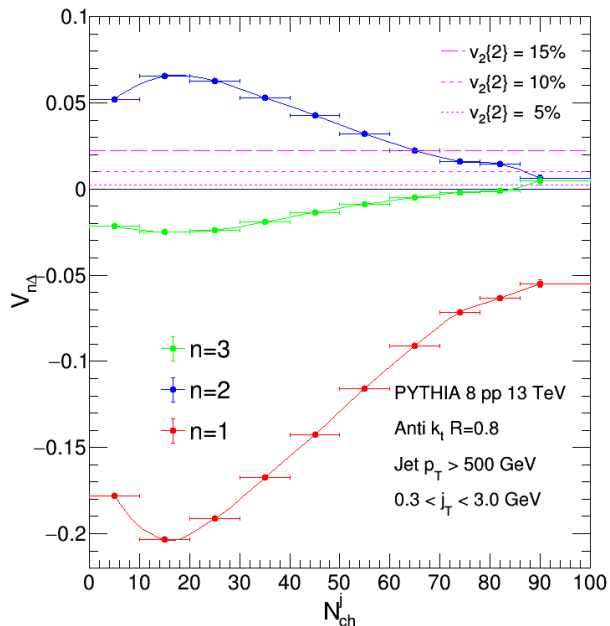


FIG. 9. The extracted two-particle Fourier coefficients,  $V_{n\Delta}$ , as a function of the charged multiplicity in jet ( $N_{\text{ch}}^j$ ), for the first three harmonic components, from AK8 jets in PYTHIA 8  $pp$  collisions at 13 TeV. The dashed lines indicate values of  $V_{2\Delta}$  equivalent to 5%, 10% and 15% in single particle  $v_2$ .

by measuring the average  $p_T$  of various particle species in a collision. Besides the average  $p_T$ , the average transverse kinetic energy,  $KE_T \equiv m_T - m = \sqrt{p_T^2 + m^2} - m$ , is also often used and has the advantage of unifying particle species of different masses (known as the “ $m_T$  scaling” [70]) in absence of the radial flow. The  $m_T$  scaling of hadron production in high-energy collisions was proposed as early as 1965 by Hagedorn based on a statistical thermodynamic approach [71]. It has been observed in minimum bias  $pp$  collisions, indicating negligible radial flow effects. In high energy  $AA$  and also high-multiplicity small systems, significant breaking of  $m_T$  scaling is observed as the multiplicity or system size increases [12, 14, 72–74].

We present the average kinetic energy,  $\langle m_T^* \rangle - m$ , calculated in the jet frame in Fig. 10, for inclusive charged hadrons, charged pions, charged kaons, protons,  $K_s^0$ ,  $\Lambda$ ,  $\Xi^-$  and  $\Omega^-$  produced within AK8 jets, for jet  $p_T > 500$  GeV as a function of charged multiplicity in jet ( $N_{\text{ch}}^j$ ) in PYTHIA 8  $pp$  events at  $\sqrt{s} = 13$  TeV. The  $m_T$  scaling is indeed present for low-multiplicity jets ( $N_{\text{ch}}^j < 10$ ) in PYTHIA 8. As  $N_{\text{ch}}^j$  increases, an increasing trend of  $\langle m_T^* \rangle - m$  is observed for all particle species but they do not appear to fall on a common trend. Instead, heavier particles appear to have greater average kinetic energy values, and by extension, greater average  $j_T$  values as well. This trend is qualitatively similar to that observed in high-multiplicity  $pp$ ,  $pA$  and  $AA$  collisions. The rate of increase of  $m_T$  with multiplicity seems greatest in the

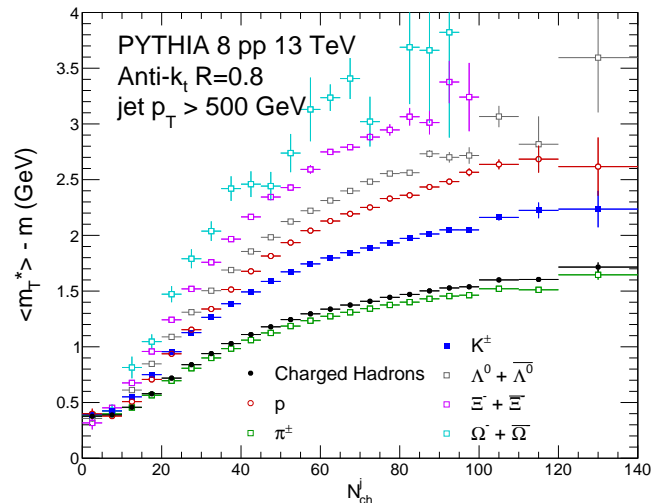


FIG. 10. The average transverse kinetic energy of various particle species produced from AK8 jets for jet  $p_T > 500$  GeV, as a function of charged multiplicity in jet ( $N_{\text{ch}}^j$ ), in PYTHIA 8  $pp$  events at  $\sqrt{s} = 13$  TeV.

range of  $N_{\text{ch}}^j \sim 20$ –30, with a flattening trend at higher multiplicities. The breakdown of  $m_T$  scaling as a function of multiplicity in PYTHIA 8 is possibly related to the color reconnection effect, which effectively generates a boost to final-state particles. Therefore, this observable alone should not be taken as a unique signature of the QGP-like state formation. Quantitative comparison with theoretical calculations, as well as supporting evidence from other observables, would be necessary to draw a conclusion.

#### D. Quantum Interference of Identical Particles

The Bose-Einstein Correlations (BEC), or interferometry exploits quantum interference effects of identical particles produced with overlapping wave functions in phase space. By studying momentum correlations of two identical bosons (fermions), an enhancement (depletion) will be observed at small momentum difference between two particles. The size of the source of particle emission at “freeze out” (when particles cease to interact) in spacial coordinate space can then be inferred from the correlation range in the momentum space. The two-particle intensity interferometry method was first invented by Hanbury, Brown and Twiss (HBT) to measure the size of astronomical objects [75]. It has since been extensively applied to extract the space-time structure of QGP in  $AA$  collisions [76–78].

In this study, the two-particle BEC correlation function is defined as the ratio,

$$C_2(\vec{q}^*) \equiv \frac{S(\vec{q}^*)}{B(\vec{q}^*)}, \quad (5)$$

where  $\vec{q}^* = \vec{p}_1^* - \vec{p}_2^*$  is the momentum difference between

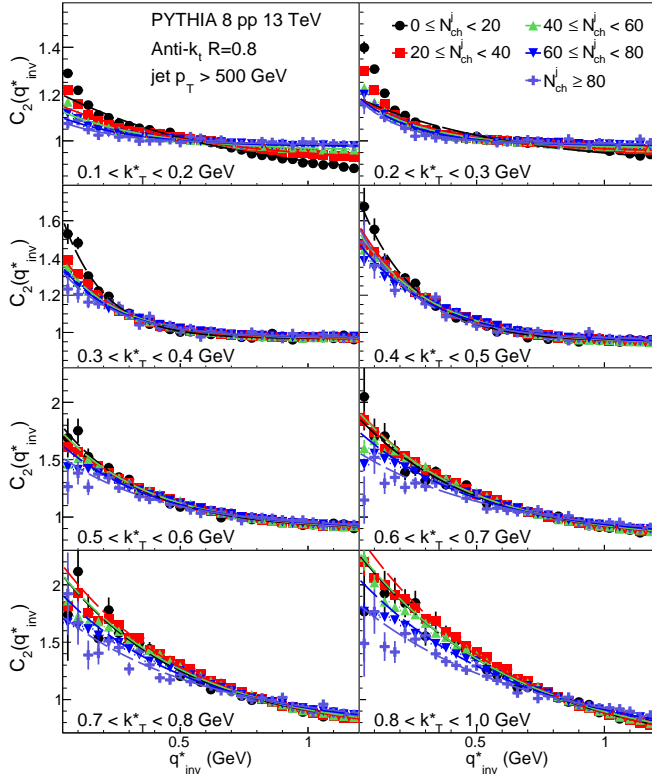


FIG. 11. The 1-D BEC correlation functions for pairs of same-sign charged pions in several ranges of charged multiplicity in jet,  $N_{\text{ch}}^j$ , for AK8 jets with jet  $p_T > 500$  GeV in PYTHIA 8  $pp$  events at  $\sqrt{s} = 13$  TeV. Each panel represents a range of pair transverse momentum  $k_T^*$ , defined in the single jet frame.

the two particles in the jet frame. Similar to two-particle angular correlations, the  $S(\vec{q}^*)$  is the measured particle pair distribution from the same jet containing potential BEC signals, while the  $B(\vec{q}^*)$  is formed with pairs of random pseudo-particles as a reference, as well as for correction of detector effects. The BEC studies can be performed in one, two or three dimensions of  $\vec{q}^*$ . For simplicity, we present a 1-D analysis in  $q_{\text{inv}}^* = |\vec{q}_1^* - \vec{q}_2^*|$  using charged pions from jets in PYTHIA 8 as a function of the charged multiplicity in jet ( $N_{\text{ch}}^j$ ) and pair transverse momentum,  $k_T^* = \frac{1}{2}|\vec{j}_{T,1} + \vec{j}_{T,2}|$ , to demonstrate the idea. No BEC signals are implemented in the PYTHIA 8 MC generator.

Figure 11 presents 1-D BEC correlation functions for pairs of same-sign charged pions in  $q_{\text{inv}}^*$  in different  $N_{\text{ch}}^j$  ranges of AK8 jets in PYTHIA 8  $pp$  events at  $\sqrt{s} = 13$  TeV. Each panel of Fig. 11 shows results for each  $k_T^*$  range.

All  $C_2(\vec{q}^*)$  distributions show a general trend of enhanced correlations toward  $q_{\text{inv}}^* \sim 0$ . This feature is qualitatively similar to those observed in  $AA$  collisions [78], where quantum interference effects are believed to play the dominant role. The width of  $C_2(\vec{q}^*)$  is inversely proportional to the size of the particle-emitting source. As mentioned earlier, there are no BEC correlations ex-

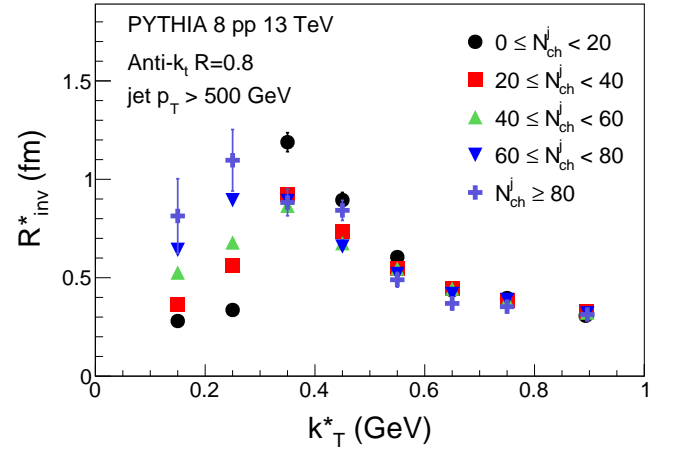


FIG. 12. The extracted 1-D BEC radii for charged pions as a function of pair transverse momentum  $k_T^*$ , defined in the single jet frame, in several ranges of charged multiplicity in jet,  $N_{\text{ch}}^j$ , for AK8 jets with jet  $p_T > 500$  GeV in PYTHIA 8  $pp$  events at  $\sqrt{s} = 13$  TeV.

pected in PYTHIA 8. Therefore, these results reflect the background contributions from the fragmentation. To distinguish the background contribution from true BEC signals, it is necessary to investigate the detailed  $N_{\text{ch}}^j$  and  $k_T^*$  dependence.

The 1-D BEC correlation function is fitted by an exponential function:

$$C \left( 1 + \lambda e^{-R_{\text{inv}}^* q_{\text{inv}}^*} \right), \quad (6)$$

where the parameter,  $R_{\text{inv}}^*$ , characterizes the size of the coherent source (in unit of fm). The extracted values of  $R_{\text{inv}}^*$  are shown in Fig. 12, as a function of  $k_T^*$ , for several  $N_{\text{ch}}^j$  ranges of AK8 jets  $p_T > 500$  GeV in PYTHIA 8  $pp$  events at  $\sqrt{s} = 13$  TeV.

In  $pp$ ,  $pA$  and  $AA$  collisions, the BEC radii parameter is observed to monotonically increase as the pair momentum decreases. This can be understood by the uncertainty principle that larger sources tend to coherently emit particles at lower momenta. The BEC radii are also found to increase with event multiplicity approximately to the power of  $1/3$ , which is again consistent with the formation of a medium that expands collectively. In the BEC analysis of particles in the jet frame using PYTHIA, shown in Fig. 12, similar features of extracted radii in  $AA$  collisions are not observed. As seen in Fig. 12, the radii parameter in the jet frame,  $R_{\text{inv}}^*$ , shows a non-monotonic behavior as a function of  $k_T^*$ , which first increases but then decreases toward low  $k_T^*$ . While the  $R_{\text{inv}}^*$  does increase with  $N_{\text{ch}}^j$  for  $k_T^* < 0.3$  GeV, this trends becomes opposite at higher  $k_T^*$ . Therefore, a systematic study of BECs for particles in high- $p_T$  jets as a function of multiplicity and pair transverse momentum in the jet frame has the potential to provide key evidence for the formation of a system with extended space-time structures.

## IV. DISCUSSIONS

In this paper, we have been focusing on studies of particles produced in inclusive single jets with high multiplicity in  $pp$  collisions at LHC energies. There are many possible extensions of proposed analyses in other directions to explore new phenomena in high density QCD physics experimentally. We discuss a few examples below.

*Thermal Photon Emission:* In  $AA$  collisions, the observation of a large excess of soft photons at low  $p_T$  ( $< 1$  GeV) over the primordial hard photon production in perturbative QCD processes [79–81] is considered as direct evidence for the formation of a thermalized QGP medium. The slope of excess photon  $p_T$  spectra provides direct information of the QGP’s temperature. If such a medium was produced in a high-multiplicity jet system, a similar enhancement of photons at small  $j_T$  inside the jet cone would also be expected. Those photons are typically identified as fragmentation photons, emitted from parton showers. Even if emitted with small  $j_T$ , these photons could still have a relatively large  $p_T$  in the laboratory reference frame, and therefore be measured by experiments like CMS and ATLAS, which have calorimeters optimized for the high- $p_T$  photon regime. However, this type of measurement will have to deal with huge backgrounds originating from hadron (e.g.  $\pi^0$ ) decays, as well as underlying event contributions and will be undoubtedly extremely challenging. At high energy lepton-lepton and lepton-hadron collisions, the underlying event background is much cleaner. Therefore, future high-energy  $e^+e^-$  colliders and the electron-ion collider planned in the USA may provide an ideal environment to search for thermal photon production from a single parton.

*Di-jets and vector boson-jet systems:* Vector boson-jet events, such as  $Z/\gamma$ -jets, in  $pp$  collisions are ideal tools to study quark propagation in the vacuum and possible collective effects developed around the quark direction of motion. All analyses performed with inclusive jets can be done with  $Z/\gamma$ -jets in the same way. A back-to-back di-jet system in  $pp$  collisions is reminiscent of the final state of  $e^+e^-$  collisions, where a color string may be stretched between the two fast-moving partons and develop interesting dynamics. Correlating particles from two different jets also helps extend the rapidity gap of two particles and benefit the search for long-range correlations. There are some complications to analyses in the di-jet system though. As the two jets are never exactly back-to-back, choosing a common  $z$  axis for the new frame (e.g., the thrust axis) may lead to some smearing if the proposed collective effects are strongest with respect to each individual jet direction. This is particularly an issue, when a hard third jet is present. More careful studies would be needed.

*Winner-take-all jet recombination:* As the first step of all proposed analyses is to rotate the lab frame to a new frame where the jet direction represents the beam axis,

the choice of the jet axis (which is not unique) plays a crucial role. Besides the standard “E-scheme” recombination [65] of jet reconstruction, where the jet axis and the jet momentum are aligned at each stage of the recursion, the “winner-take-all” scheme [82, 83] chooses the jet axis to be align with the harder particle in a pairwise recombination. The motivation of the winner-take-all scheme is to minimize the impact of soft radiation recoils to the initial parton direction. It would be interesting to investigate how all observables would depend on different choices of jet axis.

*Lepton-lepton or lepton-proton/ion collisions:* As all proposed studies take place within a single jet, they are in principle independent of the initial colliding beam species, which can be protons, leptons or ions. Therefore, these studies are highly relevant not only to the LHC but also all future high-energy colliders. In fact,  $e^+e^-$  or  $e^-p$  colliders may even provide a cleaner environment for studying high-multiplicity jets, as the underlying event contribution is much smaller.

*Jets in heavy ion collisions:* Finally, the study of parton energy loss in a QGP medium has been a main theme of research in  $AA$  collisions. In our view, a parton propagating in the vacuum or the QGP has no fundamental difference. In both cases, the parton loses its energy by interacting with other partons along its passage. The only difference is that in the QGP medium, surrounding partons are excited and thus have stronger color fields, which lead to larger energy loss than interactions with vacuum chiral condensates. Doing the same analyses for jets in heavy ion collisions may provide insights to develop a unified approach to describing parton energy loss in confined and deconfined environments.

## V. SUMMARY

Motivated by early surprises of thermal and collective phenomena in small system collisions, we postulate that non-perturbative QCD evolution of a single parton in the vacuum will develop similar long-range collective effects to those of a multi-parton system, reminiscent of what is observed in high-energy hadronic or nuclear interactions with high-multiplicity final-state particles. We propose searches for these properties of a single parton propagating in the vacuum using high- $p_T$  jets produced with high multiplicities in high-energy elementary collisions, e.g., at the LHC. A set of observables are studied in detail using the PYTHIA 8 Monte Carlo event generator, where no collective effects are expected inside the jet. Experimental observation of the proposed effects (e.g., long-range collectivity or strangeness enhancement) in a single jet will offer a new view of non-perturbative QCD dynamics of multi-parton systems at the smallest scales. On the other hand, absence of these effects may offer new insights in to the role of quantum entanglement in the observed thermal behavior of particle production in high energy collisions.

This work is in part supported by the Department of

Energy grant number DE-SC0005131.

- 
- [1] D. J. Gross and F. Wilczek, *Phys. Rev. Lett.* **30**, 1343 (1973).
- [2] H. Politzer, *Phys. Rev. Lett.* **30**, 1346 (1973).
- [3] R. Brock *et al.* (CTEQ), *Rev. Mod. Phys.* **67**, 157 (1995).
- [4] B. Andersson, G. Gustafson, G. Ingelman, and T. Sjstrand, *Phys. Rept.* **97**, 31 (1983).
- [5] G. Marchesini, B. Webber, G. Abbiendi, I. Knowles, M. Seymour, and L. Stanco, *Comput. Phys. Commun.* **67**, 465 (1992).
- [6] R. Kogler *et al.*, *Rev. Mod. Phys.* **91**, 045003 (2019), arXiv:1803.06991 [hep-ex].
- [7] F. Karsch, *Nucl. Phys. A* **590**, 367C (1995), arXiv:hep-lat/9503010 [hep-lat].
- [8] F. Karsch, *Lect. Notes Phys.* **583**, 209 (2002), arXiv:hep-lat/0106019 [hep-lat].
- [9] A. Bazavov *et al.* (HotQCD), *Phys. Lett. B* **795**, 15 (2019), arXiv:1812.08235 [hep-lat].
- [10] “CERN Press Release Feb. 10,” (2020).
- [11] I. Arsene *et al.* (BRAHMS), *Nucl. Phys. A* **757**, 1 (2005), arXiv:nucl-ex/0410020 [nucl-ex].
- [12] K. Adcox *et al.* (PHENIX), *Nucl. Phys. A* **757**, 184 (2005), arXiv:nucl-ex/0410003 [nucl-ex].
- [13] B. B. Back *et al.* (PHOBOS), *Nucl. Phys. A* **757**, 28 (2005), arXiv:nucl-ex/0410022 [nucl-ex].
- [14] J. Adams *et al.* (STAR), *Nucl. Phys. A* **757**, 102 (2005), arXiv:nucl-ex/0501009 [nucl-ex].
- [15] B. Muller, J. Schukraft, and B. Wyslouch, *Ann. Rev. Nucl. Part. Sci.* **62**, 361 (2012), arXiv:1202.3233 [hep-ex].
- [16] J. Adams *et al.* (STAR), *Phys. Rev. Lett.* **95**, 152301 (2005), nucl-ex/0501016.
- [17] B. Alver *et al.* (PHOBOS), *Phys. Rev. C* **81**, 024904 (2010), arXiv:0812.1172 [nucl-ex].
- [18] B. Abelev *et al.* (STAR), *Phys. Rev. C* **80**, 064912 (2009), arXiv:0909.0191 [nucl-ex].
- [19] B. Alver *et al.* (PHOBOS), *Phys. Rev. Lett.* **104**, 062301 (2010), arXiv:0903.2811 [nucl-ex].
- [20] S. Chatrchyan *et al.* (CMS), *JHEP* **07**, 076 (2011), arXiv:1105.2438 [nucl-ex].
- [21] S. Chatrchyan *et al.* (CMS), *Eur. Phys. J. C* **72**, 2012 (2012), arXiv:1201.3158 [nucl-ex].
- [22] K. Aamodt *et al.* (ALICE), *Phys. Rev. Lett.* **105**, 252302 (2010), arXiv:1011.3914 [nucl-ex].
- [23] G. Aad *et al.* (ATLAS), *Phys. Rev. C* **86**, 014907 (2012), arXiv:1203.3087 [hep-ex].
- [24] S. Chatrchyan *et al.* (CMS), *JHEP* **02**, 088 (2014), arXiv:1312.1845 [nucl-ex].
- [25] J.-Y. Ollitrault, *Phys. Rev. D* **46**, 229 (1992).
- [26] D. Teaney, *Phys. Rev. C* **68**, 034913 (2003), arXiv:nucl-th/0301099.
- [27] P. Romatschke and U. Romatschke, *Phys. Rev. Lett.* **99**, 172301 (2007), arXiv:0706.1522 [nucl-th].
- [28] U. Heinz and R. Snellings, *Ann. Rev. Nucl. Part. Sci.* **63**, 123 (2013), arXiv:1301.2826 [nucl-th].
- [29] C. Gale, S. Jeon, and B. Schenke, *Int. J. Mod. Phys. A* **28**, 1340011 (2013), arXiv:1301.5893 [nucl-th].
- [30] V. Khachatryan *et al.* (CMS), *JHEP* **09**, 091 (2010), arXiv:1009.4122 [hep-ex].
- [31] G. Aad *et al.* (ATLAS), *Phys. Rev. Lett.* **116**, 172301 (2016), arXiv:1509.04776 [hep-ex].
- [32] V. Khachatryan *et al.* (CMS), *Phys. Rev. Lett.* **116**, 172302 (2016), arXiv:1510.03068 [nucl-ex].
- [33] V. Khachatryan *et al.* (CMS), *Phys. Lett. B* **765**, 193 (2017), arXiv:1606.06198 [nucl-ex].
- [34] G. Aad *et al.* (ATLAS), *Phys. Rev. Lett.* **124**, 082301 (2020), arXiv:1909.01650 [nucl-ex].
- [35] W. Li, *Mod. Phys. Lett. A* **27**, 1230018 (2012), arXiv:1206.0148 [nucl-ex].
- [36] S. Chatrchyan *et al.* (CMS), *Phys. Lett. B* **718**, 795 (2013), arXiv:1210.5482 [nucl-ex].
- [37] B. Abelev *et al.* (ALICE), *Phys. Lett. B* **719**, 29 (2013), arXiv:1212.2001 [nucl-ex].
- [38] G. Aad *et al.* (ATLAS), *Phys. Rev. Lett.* **110**, 182302 (2013), arXiv:1212.5198 [hep-ex].
- [39] R. Aaij *et al.* (LHCb), *Phys. Lett. B* **762**, 473 (2016), arXiv:1512.00439 [nucl-ex].
- [40] B. B. Abelev *et al.* (ALICE), *Phys. Lett. B* **726**, 164 (2013), arXiv:1307.3237 [nucl-ex].
- [41] V. Khachatryan *et al.* (CMS), *Phys. Lett. B* **742**, 200 (2015), arXiv:1409.3392 [nucl-ex].
- [42] V. Khachatryan *et al.* (CMS), *Phys. Rev. Lett.* **115**, 012301 (2015), arXiv:1502.05382 [nucl-ex].
- [43] M. Aaboud *et al.* (ATLAS), *Eur. Phys. J. C* **77**, 428 (2017), arXiv:1705.04176 [hep-ex].
- [44] M. Aaboud *et al.* (ATLAS), *Phys. Rev. C* **97**, 024904 (2018), arXiv:1708.03559 [hep-ex].
- [45] C. Aidala *et al.* (PHENIX), *Nature Phys.* **15**, 214 (2019), arXiv:1805.02973 [nucl-ex].
- [46] L. Adamczyk *et al.* (STAR), *Phys. Lett. B* **747**, 265 (2015), arXiv:1502.07652 [nucl-ex].
- [47] A. Adare *et al.* (PHENIX), *Phys. Rev. Lett.* **115**, 142301 (2015), arXiv:1507.06273 [nucl-ex].
- [48] C. Aidala *et al.* (PHENIX), *Phys. Rev. Lett.* **120**, 062302 (2018), arXiv:1707.06108 [nucl-ex].
- [49] K. Dusling, W. Li, and B. Schenke, *Int. J. Mod. Phys. E* **25**, 1630002 (2016), arXiv:1509.07939 [nucl-ex].
- [50] J. L. Nagle and W. A. Zajc, *Ann. Rev. Nucl. Part. Sci.* **68**, 211 (2018), arXiv:1801.03477 [nucl-ex].
- [51] B. Schenke, C. Shen, and P. Tribedy, *Phys. Rev. C* **102**, 044905 (2020), arXiv:2005.14682 [nucl-th].
- [52] F. Becattini, *Z. Phys. C* **69**, 485 (1996).
- [53] F. Becattini, P. Castorina, J. Manninen, and H. Satz, *Eur. Phys. J. C* **56**, 493 (2008), arXiv:0805.0964 [hep-ph].
- [54] P. Castorina, D. Kharzeev, and H. Satz, *Eur. Phys. J. C* **52**, 187 (2007), arXiv:0704.1426 [hep-ph].
- [55] P. Braun-Munzinger, J. Stachel, J. P. Wessels, and N. Xu, *Phys. Lett. B* **344**, 43 (1995), arXiv:nucl-th/9410026 [nucl-th].
- [56] A. Badea, A. Baty, P. Chang, G. M. Innocenti, M. Maggi, C. McGinn, M. Peters, T.-A. Sheng, J. Thaler, and Y.-J. Lee, *Phys. Rev. Lett.* **123**, 212002 (2019), arXiv:1906.00489 [hep-ex].
- [57] I. Abt *et al.* (ZEUS), “Two-particle azimuthal correlations as a probe of collective behaviour in deep inelastic ep scattering at HERA,” (2019), arXiv:1912.07431 [hep-ex].
- [58] S. Hawking, *Commun. Math. Phys.* **43**, 199 (1975), [Er-

- ratum: Commun.Math.Phys. 46, 206 (1976)].
- [59] W. Unruh, *Phys. Rev. D* **14**, 870 (1976).
  - [60] D. E. Kharzeev and E. M. Levin, *Phys. Rev. D* **95**, 114008 (2017), [arXiv:1702.03489 \[hep-ph\]](#).
  - [61] J. Berges, S. Floerchinger, and R. Venugopalan, *Phys. Lett. B* **778**, 442 (2018), [arXiv:1707.05338 \[hep-ph\]](#).
  - [62] A. M. Kaufman, M. E. Tai, A. Lukin, M. Rispoli, R. Schittko, P. M. Preiss, and M. Greiner, *Science* **353**, 794 (2016).
  - [63] O. K. Baker and D. E. Kharzeev, *Phys. Rev. D* **98**, 054007 (2018), [arXiv:1712.04558 \[hep-ph\]](#).
  - [64] Z. Tu, D. E. Kharzeev, and T. Ullrich, *Phys. Rev. Lett.* **124**, 062001 (2020), [arXiv:1904.11974 \[hep-ph\]](#).
  - [65] M. Cacciari, G. P. Salam, and G. Soyez, *JHEP* **04**, 063 (2008), [arXiv:0802.1189 \[hep-ph\]](#).
  - [66] T. Sjostrand, S. Mrenna, and P. Z. Skands, *Comput. Phys. Commun.* **178**, 852 (2008), [arXiv:0710.3820 \[hep-ph\]](#).
  - [67] G. Aad *et al.* (ATLAS), *Eur. Phys. J. C* **76**, 322 (2016), [arXiv:1602.00988 \[hep-ex\]](#).
  - [68] P. Koch, B. Muller, and J. Rafelski, *Phys. Rept.* **142**, 167 (1986).
  - [69] J. Adam *et al.* (ALICE), *Nature Phys.* **13**, 535 (2017), [arXiv:1606.07424 \[nucl-ex\]](#).
  - [70] G. Gatoff and C. Y. Wong, *Phys. Rev. D* **46**, 997 (1992).
  - [71] R. Hagedorn, *Nuovo Cim. Suppl.* **3**, 147 (1965).
  - [72] V. Khachatryan *et al.* (CMS), *Phys. Lett. B* **768**, 103 (2017), [arXiv:1605.06699 \[nucl-ex\]](#).
  - [73] S. Acharya *et al.* (ALICE), *Eur. Phys. J. C* **80**, 693 (2020), [arXiv:2003.02394 \[nucl-ex\]](#).
  - [74] B. B. Abelev *et al.* (ALICE), *Phys. Lett. B* **728**, 25 (2014), [arXiv:1307.6796 \[nucl-ex\]](#).
  - [75] R. Hanbury Brown and R. Q. Twiss, *Nature* **178**, 1046 (1956).
  - [76] W. A. Zajc *et al.*, *Phys. Rev. C* **29**, 2173 (1984).
  - [77] U. W. Heinz and B. V. Jacak, *Ann. Rev. Nucl. Part. Sci.* **49**, 529 (1999), [arXiv:nucl-th/9902020](#).
  - [78] M. A. Lisa, S. Pratt, R. Soltz, and U. Wiedemann, *Ann. Rev. Nucl. Part. Sci.* **55**, 357 (2005), [arXiv:nucl-ex/0505014](#).
  - [79] A. Adare *et al.* (PHENIX), *Phys. Rev. Lett.* **104**, 132301 (2010), [arXiv:0804.4168 \[nucl-ex\]](#).
  - [80] J. Adam *et al.* (ALICE), *Phys. Lett. B* **754**, 235 (2016), [arXiv:1509.07324 \[nucl-ex\]](#).
  - [81] L. Adamczyk *et al.* (STAR), *Phys. Lett. B* **770**, 451 (2017), [arXiv:1607.01447 \[nucl-ex\]](#).
  - [82] D. Bertolini, T. Chan, and J. Thaler, *JHEP* **04**, 013 (2014), [arXiv:1310.7584 \[hep-ph\]](#).
  - [83] A. J. Larkoski, D. Neill, and J. Thaler, *JHEP* **04**, 017 (2014), [arXiv:1401.2158 \[hep-ph\]](#).